Chemical Control of Superparamagnetic Properties of Magnesium and Cobalt Spinel Ferrite Nanoparticles through Atomic Level Magnetic Couplings

Chao Liu, Bingsuo Zou,† Adam J. Rondinone, and Z. John Zhang*

Contribution from the School of Chemistry & Biochemistry, Georgia Institute of Technology, Atlanta, Georgia 30332-0400

Received March 3, 2000

Abstract: A correlation between the electron spin−orbital angular momentum coupling and the superparamagnetic properties has been established in $MgFe_2O_4$ and $CoFe_2O_4$ spinel ferrite nanoparticles. The contribution to the magnetic anisotropy from the Fe^{3+} lattice sites is almost the same in both nanocrystallites as neutron diffraction studies have shown a similar cation distribution in these two types of spinel ferrite nanoparticles. Due to the strong magnetic couplings from Co^{2+} lattice sites, the blocking temperature of $CoFe_2O_4$ nanoparticles is at least 150 deg higher than the same sized $MgFe_2O_4$ nanoparticles. Mössbauer spectroscopy studies demonstrate that the magnetic anisotropy of $CoFe_2O_4$ nanoparticles is higher than that of the same size $MgFe_2O_4$ nanoparticles. These studies indicate that the superparamagnetic properties of nanoparticles can be controlled through chemically adjusting the magnetic anisotropy energy.

Introduction

Magnetic properties of materials originate from the quantum couplings at the atomic level including the coupling between electron spins (S−S coupling) and the coupling between electron spin and the angular momentum of the electron orbital (L−S coupling). The magnetic moments are separated into several domains upon spontaneous magnetization in a bulk single crystal as a consequence of minimizing the total magnetic energy in the crystal. Different domains have different magnetization directions and are separated by domain walls. When the magnetization by an external magnetic field occurs, the domain walls move across the crystal and the whole crystal eventually changes from a multidomain magnetic structure to a single domain with all the magnetic moments pointing to the field direction. The readiness of domain wall displacement has a dominant effect to the magnetic properties of bulk materials. Domain wall displacement is very complex. In addition to the intrinsic factor of magnetocrystalline anisotropy, which comes from L−S coupling in materials, domain wall displacement is greatly affected by many extrinsic factors including defects, lattice strains, and chemical impurity. Due to the inevitable existence of these extrinsic factors in bulk magnetic materials, it is rather difficult to correlate the magnetic properties with the magnetic couplings in bulk materials.

Each of the magnetic nanoparticles usually possesses a single magnetic domain. Therefore, the nanoparticles offer excellent opportunities for the fundamental studies on the relationship between magnetic behavior and magnetic couplings at the atomic level. An elucidating example is the correlation between the L−S coupling and the superparamagnetic properties of nanoparticles through the variation of magnetic anisotropy. Superparamagnetism is a unique feature of magnetic nanoparticles. It is of great fundamental interest such as macroscopic quantum tunneling (MQT),[1,2] and also of essential importance to the technological applications of magnetic nanoparticles including high-density data storage,[3] contrast enhancement of magnetic resonance imaging (MRI),[4] and magnetic carriers for site-specific drug delivery.[5] Moreover, the correlation between magnetic coupling and superparamagnetism in nanoparticles elucidates the quantum origin of the magnetic properties and may provide the insight for the advancement of magnetoelectronics.[6]

Superparamagnetic properties of nanoparticles are determined by the magnetocrystalline anisotropy, which comes from the L−S couplings at crystal lattices. According to the Stoner−Wohlfarth theory, the magnetocrystalline anisotropy E_A of a single-domain particle can be approximated as:

$$E_A = KV \sin^2\theta \tag{1}$$

where K is the magnetocrystalline anisotropy constant, V is the volume of the nanoparticle, and θ is the angle between the magnetization direction and the easy axis of the nanoparticle.[7] In magnetic nanoparticles with a spherical shape, the magnetocrystalline anisotropy can be approximated as the total magnetic anisotropy.[8] The magnetic anisotropy E_A serves as an energy barrier for blocking the flips of magnetic moments. When E_A becomes comparable with thermal activation energy, k_BT with k_B as the Boltzmann constant, thermal activation

* To whom correspondence should be addressed.
† Permanent address: Institute of Physics, Chinese Academy of Sciences, Beijing 100080, China.

(1) Awschalom, D. D.; DiVincenzo, D. P. *Phys. Today* **1995**, *48* (4), 43.
(2) Tejada, J.; Ziolo, R. F.; Zhang, X. X. *Chem. Mater*. **1996**, *8*, 1784.
(3) Kryder, M. H. *MRS Bull.* **1996**, *21* (9) 17.
(4) Mitchell, D. G. *J. Magn. Reson. Imaging* **1997**, *7*, 1.
(5) Häfeli, U.; Schütt, W.; Teller, J.; Zborowski, M., Eds. *Scientific and Clinical Applications of Magnetic Carriers*; Plenum: New York, 1997.
(6) Prinz, G. A. *Science* **1998**, *282*, 1660.
(7) Stoner, E. C.; Wohlfarth, E. P. *Philos. Trans. R. Soc. A* **1948**, *240*, 599; reprinted in *IEEE Trans. Magn*. **1991**, *27*, 3475.
(8) Moumen, N.; Bonville, P.; Pileni, M. P. *J. Phys. Chem*. **1996**, *100*, 14410.

10.1021/ja000784g CCC: $19.00
Published on Web 06/16/2000

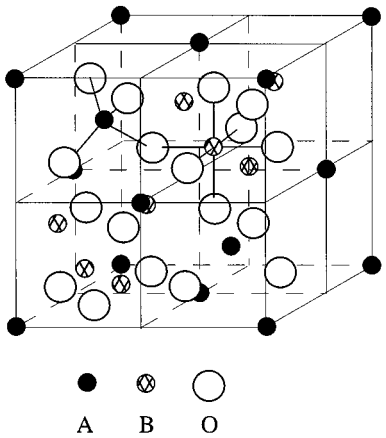

Figure 1. A schematic diagram for a partially filled unit cell of spinel AB_2O_4.

can overcome the anisotropy energy barrier and the nanoparticles become superparamagnetic with the magnetization direction randomly flipping.

The superparamagnetic state plays drastically different roles in various technological applications of magnetic nanoparticles. The nanoparticles at the superparamagnetic state are essential for applications such as MRI contrast enhancement agents or magnetic carriers for drug delivery. On the other hand, avoiding the superparamagnetic state is vital for maintaining the thermal stability of magnetic data bits in high-density information storage. The superparamagnetic properties of nanoparticles can be controlled by adjusting E_A. Through a well-controlled E_A, we can design and control the superparamagnetic properties of nanoparticles for each of the specific applications.

E_A will change when the size of the nanoparticles V and/or the anisotropy constant K varies. Since K is determined by the strength of the L−S couplings, it directly reflects the correlation between the L−S coupling and the superparamagnetic properties of nanoparticles. The superparamagnetic properties of spinel ferrite nanoparticles are excellent cases to correlate with the L−S couplings at the lattices of spinel crystal. Spinel ferrite has a general chemical composition of MFe_2O_4 (M = Mn, Mg, Zn, Ni, Co, Fe, etc.).[9] It has a face-centered cubic structure with a large unit cell containing eight formula units. There are two kinds of lattices for cation occupancy. A and B sites have tetrahedral and octahedral coordinations, respectively (Figure 1). Commonly, the M^{2+} and Fe^{3+} cations distribute at both sites. Since the $Fe^{3+}{}_A-Fe^{3+}{}_B$ superexchange interaction is normally different from the $M^{2+}{}_A-Fe^{3+}{}_B$ interaction, variation of the cation distribution over the A and B sites in the spinel leads to different magnetic properties of these oxides even though the chemical composition of the compound does not change.[10]

A few types of spinel ferrite nanoparticles such as $CoFe_2O_4$, $MnFe_2O_4$, and $MgFe_2O_4$ have been synthesized in our laboratory and other laboratories by using the coprecipitation or microemulsion method.[10−17] Some size-dependent superparamagnetic properties have been reported.[18−23] However, these superparamagnetic properties have not been systematically correlated with the atomic-level magnetic interactions even though the magnetic properties of nanoparticles originate from the quantum couplings at the atomic level.

We report here a direct correlation between the electron spin−orbital angular momentum (L−S) coupling and the superparamagnetic properties of $MgFe_2O_4$ and $CoFe_2O_4$ spinel ferrite nanoparticles. Due to the strong magnetic couplings from Co^{2+} lattice sites, the blocking temperature of $CoFe_2O_4$ nanoparticles is at least 150 deg higher than that of the same sized $MgFe_2O_4$ nanoparticles. Mössbauer spectroscopy studies demonstrate that the magnetic anisotropy of $CoFe_2O_4$ nanoparticles is higher than that of the same sized $MgFe_2O_4$ nanoparticles.

Experimental Section

Synthesis of Magnetic Nanoparticles. $MgFe_2O_4$ and $CoFe_2O_4$ nanoparticles used to study the correlation between the L−S coupling and the superparamagnetic properties of nanoparticles have been synthesized by using normal micelle and reverse micelle methods.[11] $MgFe_2O_4$ nanoparticles have been synthesized from water-in-toluene reverse micelles using sodium dodecylbenzenesulfonate (NaDBS) $[CH_3(CH_2)_{11}(C_6H_4)SO_3]Na$ and cetyltrimethylammonium bromide (CTAB) $[CH_3(CH_2)_{15}N(CH_3)_3]Br$ as surfactants. $CoFe_2O_4$ nanoparticles have been synthesized from normal micelles formed by sodium dodecyl sulfate (NaDS) $[CH_3(CH_2)_{10}CH_2OSO_3]Na$ surfactant.

Magnetic Measurement. The magnetic properties of the nanoparticles have been measured by using a Quantum Design MPMS-5S SQUID magnetometer with a magnetic field up to 5 T.

Transmission Electron Microscopy. Transmission electron microscopy (TEM) studies have been performed using a Hitachi HF-2000 field-emission transmission electron microscope. The nanoparticles were dispersed on holey carbon grids for TEM observation.

Neutron Diffraction. Neutron diffraction data were collected using the HB4 powder diffractometer at the High-Flux Isotope Reactor (HFIR) of Oak Ridge National Laboratory. Details can be found in ref 10.

Mössbauer Spectroscopy. The superparamagnetic relaxation behavior of magnetic nanoparticles was studied with ^{57}Fe Mössbauer spectroscopy by using an Austin S-600 Mössbauer Spectrometer (Austin Science Associates Inc.). A triangular waveform was employed to drive the linear motor in a constant acceleration mode. Experiment temperatures were controlled by Janis SVT Research Cryostat System for studies below room temperature. A VF-1000 Vacuum Furnace was used for studies above room temperature. MOSMOD Mössbauer Analysis Software was used to analyze the data.

Results and Discussion

The X-ray powder diffraction studies have shown that the synthesized magnetic nanoparticles have a single spinel phase. The lattice constants are 8.3954 and 8.3816 Å for the $MgFe_2O_4$ and $CoFe_2O_4$ nanoparticles, respectively. The average size of $MgFe_2O_4$ nanoparticles can be controlled from 2 to 45 nm, and the mean size of $CoFe_2O_4$ nanoparticles can be varied from 2 to 35 nm. The size distributions for the $MgFe_2O_4$ and $CoFe_2O_4$ nanoparticles are less than 25% and 15%, respectively. Figure 2a shows some typical $MgFe_2O_4$ nanoparticles with a diameter

(9) McCurrie, R. A. *Ferromagnetic Materials—Structure and Properties*; Academic: London, 1994.
(10) Zhang, Z. J.; Wang, Z. L.; Chakoumakos, B. C.; Yin, J. S. *J. Am. Chem. Soc.* **1998**, *120*, 1800.
(11) Rondinone, A. J.; Samia, A. C. S.; Zhang, Z. J. *J. Phys. Chem. B* **1999**, *103*, 6876.
(12) Liu, C.; Zou, B.; Rondinone, A. J.; Zhang, Z. J. *J. Phys. Chem. B* **2000**, *104*, 1141.
(13) Chen, Q.; Rondinone, A. J.; Chakoumakos, B. C.; Zhang, Z. J. *J. Magn. Magn. Mater.* **1999**, *194*, 1.
(14) Moumen, N.; Pileni, M. P. *Chem. Mater.* **1996**, *8*, 1128.
(15) Pileni, M. P.; Moumen, N. *J. Phys. Chem.* **1996**, *100*, 1867.
(16) Tang, Z. X.; Sorensen, C. M.; Klabunde, K. J.; Hadjipanayis, G. C. *J. Colloid Interface Sci.* **1991**, *146*, 38.
(17) Seip, C. T.; Carpenter, E. E.; O'Connor, C. J.; John, V. T.; Li, S. *IEEE Trans. Magn.* **1998**, *34*, 1111.
(18) Chen, Q.; Zhang, Z. J. *Appl. Phys. Lett.* **1998**, *73*, 3156.
(19) Tang, Z. X.; Sorensen, C. M.; Klabunde, K J.; Hadjipanayis, G. C. *Phys. Rev. Lett.* **1991**, *67*, 3602.
(20) Kulkarni, G. U.; Kannan, K. R.; Arunarkavalli, T.; Rao, C. N. R. *Phys. Rev. B* **1994**, *49*, 724.
(21) Van der Zaag, P. J.; Noordermeer, A.; Johnson, M. T.; Bongers, P. E. *Phys. Rev. Lett.* **1992**, *68*, 3112.
(22) Brabers, V. A. M. *Phys. Rev. Lett.* **1992**, *68*, 3113.
(23) Chen, J. P.; Sorensen, C. M.; Klabunde, K. J.; Hadjipanayis, G. C.; Devlin, E.; Kostikas, A. *Phys. Rev. B* **1996**, *54*, 9288.

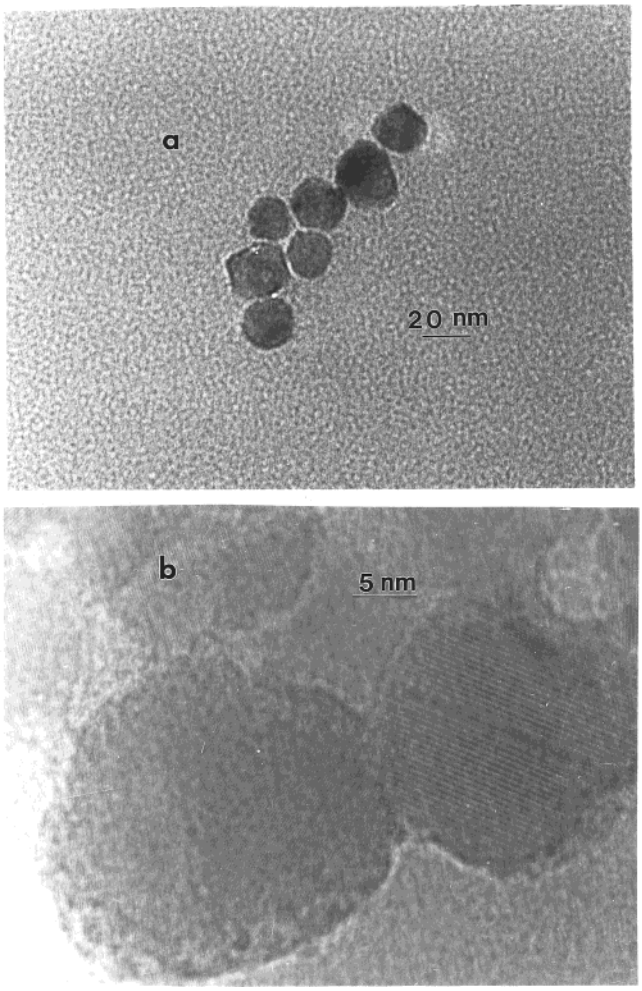

Figure 2. (a) Transmission electron micrograph of some typical $MgFe_2O_4$ nanoparticles with a diameter around 20 nm. (b) The high-resolution image of a nanoparticle in a bright field.

around 20 nm. High-resolution transmission electron microscopy (Figure 2b) and electron diffraction studies confirm that these nanoparticles are single crystals with no evidence indicating the existence of defects such as grain boundary, dislocation, and stacking fault. Chemical analysis using the inductively coupled plasma (ICP) method has shown that the composition ratio of Mg:Fe is 1:2 and so is the Co:Fe ratio. Mössbauer spectroscopy studies have proved that the Fe cations in both $MgFe_2O_4$ and $CoFe_2O_4$ nanoparticles have a +3 oxidation state, which indicates that our nanoparticles have a stoichiometry close to a standard spinel with four oxygens per formula.

Figure 3 shows the zero-field-cooled magnetization of the $MgFe_2O_4$ nanoparticles with diameters over a large range. As Figure 3 displays for various size $MgFe_2O_4$ nanoparticles, the magnetization shows a maximum value at certain temperatures for each size of nanoparticle. Afterward, the magnetization decreases and shows a paramagnetic behavior. The temperature associated with the maximum magnetization increases with increasing size of the nanoparticles. Such temperature-dependent magnetization is a characteristic feature of superparamagnetism. Neutron diffraction studies have been carried out to confirm that a magnetic order exists in the nanoparticles showing paramagnetic behavior. The temperatures at which the nanoparticles show the maximum magnetization are the blocking temperatures T_b of the corresponding nanoparticles.

Similar magnetization measurements have been conducted on $CoFe_2O_4$ nanoparticles. The magnetizations of various sized

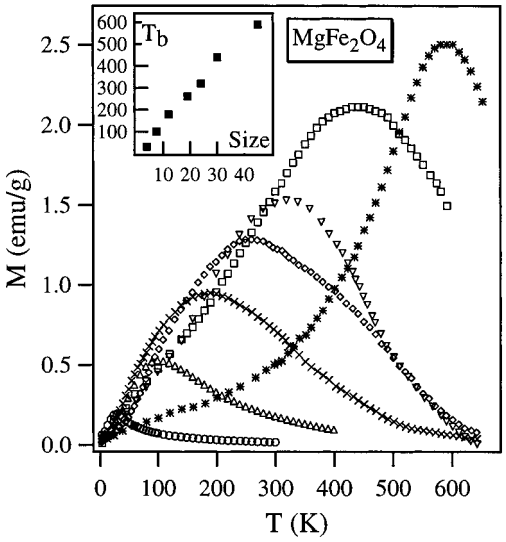

Figure 3. Magnetization vs temperature for $MgFe_2O_4$ nanoparticles with various sizes (○, 4.0 nm; △, 7.5 nm; ×, 12 nm; ◇, 19 nm; □, 24 nm; ▽, 30 nm; *, 45 nm) under a 100 G magnetic field. The inset shows the correlation between the blocking temperature and nanoparticle mean diameter.

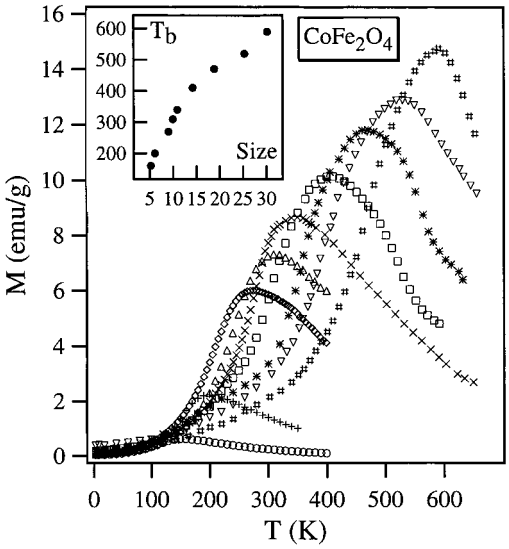

Figure 4. Magnetization vs temperature for $CoFe_2O_4$ nanoparticles with various sizes (○, 5.2 nm; +, 6.1 nm; ◇, 9.0 nm; △, 9.9 nm; ×, 10.9 nm; □, 14.2 nm; *, 18.8 nm; ▽, 25.3 nm; #, 30.2 nm) under a 100 G magnetic field. The inset shows the correlation between the blocking temperature and nanoparticle mean diameter.

$CoFe_2O_4$ nanoparticles are shown in Figure 4 as a function of temperature. $CoFe_2O_4$ nanoparticles also show the superparamagnetic behavior with the maximum magnetization occurring at the blocking temperature. The blocking temperature of $CoFe_2O_4$ nanoparticles also increases with increasing size of the nanoparticles.

The superparamagnetic properties of $MgFe_2O_4$ and $CoFe_2O_4$ nanoparticles clearly show that the magnetocrystalline anisotropy E_A of the nanoparticles is a key parameter. The height of E_A decides the temperature range in which the thermal activation overcomes E_A and the nanoparticles show a superparamagnetic behavior. The relationship between the blocking temperature and the nanoparticle size reflects clearly the size dependence of E_A. Although the blocking temperature increases with increasing size in both $MgFe_2O_4$ and $CoFe_2O_4$ nanoparticles, T_b of $CoFe_2O_4$ nanoparticles is located in a much higher

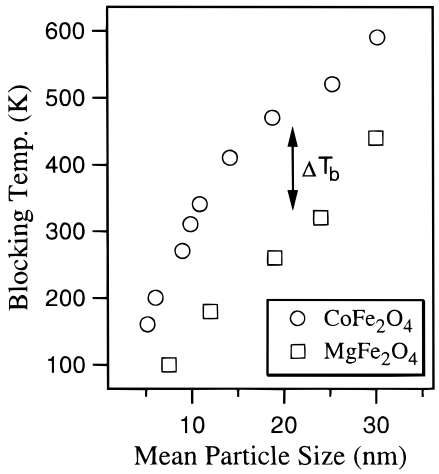

Figure 5. Comparison of the blocking temperatures in the same size $MgFe_2O_4$ and $CoFe_2O_4$ nanoparticles.

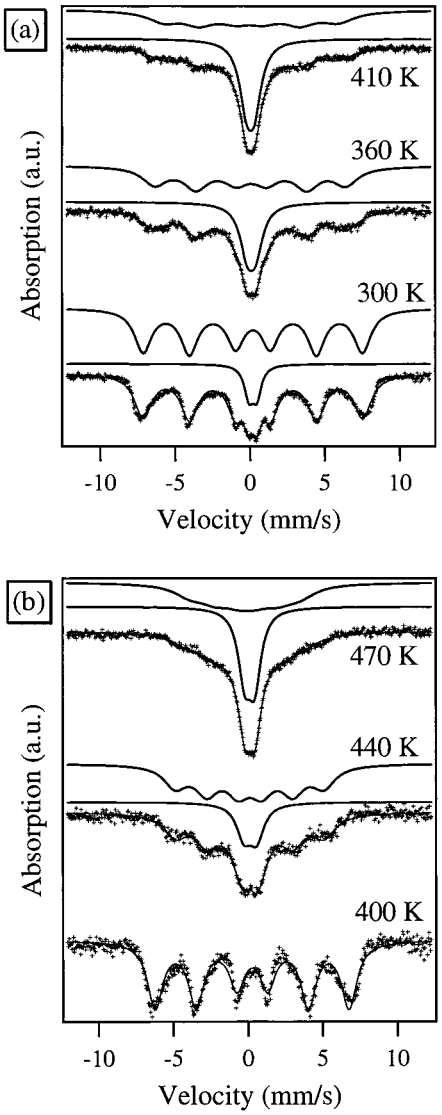

Figure 6. Temperature dependence of Mössbauer spectra of 20 nm $MgFe_2O_4$ (a) and $CoFe_2O_4$ (b) nanoparticles.

temperature range. Figure 5 shows that the blocking temperature of $CoFe_2O_4$ nanoparticles is at least 150 deg higher than that for $MgFe_2O_4$ nanoparticles of the same size. Higher T_b indicates that E_A is much higher in $CoFe_2O_4$ nanoparticles compared to

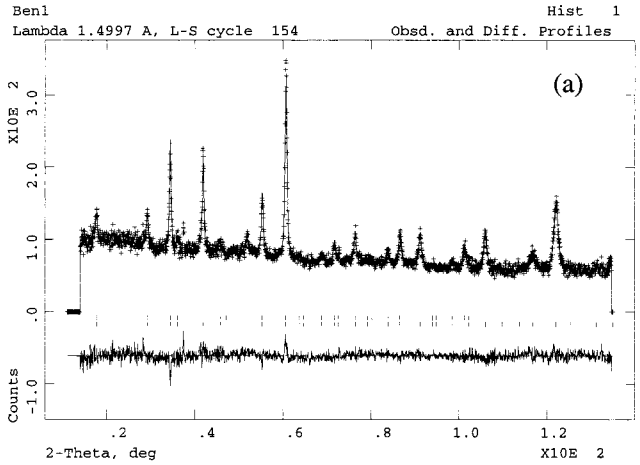

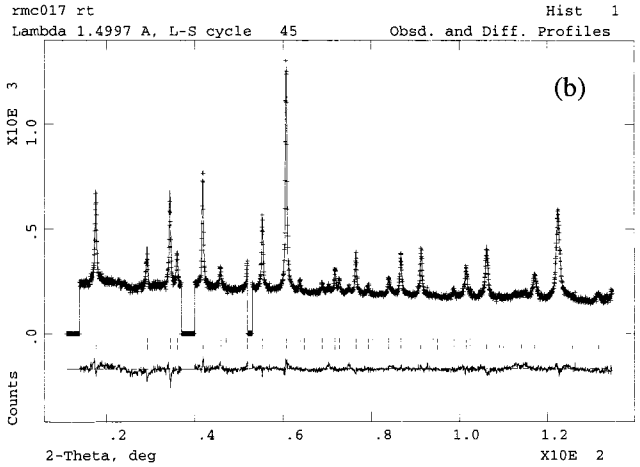

Figure 7. Neutron diffraction patterns of $MgFe_2O_4$ (a) and $CoFe_2O_4$ (b) nanoparticles at room temperature. The wavelength of the neutron beam is 1.4997 Å. Below the pattern, the first row of sticks marks the peaks from the magnetic scattering of $CoFe_2O_4$ nanoparticles and the second row of sticks corresponds to the peaks from the nuclear scattering. The excluded regions (downward sparks) eliminate the diffraction peaks of the Nb heating element of the furnace.

the same sized $MgFe_2O_4$ nanoparticles. Since the arrangement of the easy axes relative to the field direction should also be the same in both randomly oriented $MgFe_2O_4$ and $CoFe_2O_4$ nanoparticles, the higher E_A suggests that the anisotropy constant K is larger in $CoFe_2O_4$ nanoparticles as eq 1 implies.

Mössbauer spectroscopy studies have been carried out to confirm the large difference in the anisotropy constant K between $MgFe_2O_4$ and $CoFe_2O_4$ nanoparticles. The measurement time in Mössbauer spectroscopy is equal to the Larmor precession period of the nucleus, which is about 10 ns for ^{57}Fe.[24−26] This time scale can be used to observe how fast the magnetization direction flips in superparamagnetic nanoparticles. The reorientation time τ of magnetization is related to the anisotropy constant K and nanoparticle size as well as measuring temperature through the Néel equation:

$$\tau = \tau_o \exp(KV/k_B T) \qquad (2)$$

where τ_o is a constant. If the magnetization direction of the

(24) Aharoni, A. *Phys. Rev. B* **1973**, *7*, 1103.
(25) Hoy, G. R. In *Mössbauer Spectroscopy Applied to Inorganic Chemistry*; Long, G. J., Ed.; Plenum Press: New York, 1984; Vol. 1, p 195.
(26) Morup, S. *Hyperfine Interact.* **1990**, *60*, 959.

Table 1. Characteristic Structural and Magnetic Parameters Determined from the Reitveld Refinement of Neutron Diffraction for $(Co_xFe_{1-x})[Co_{1-x}Fe_{1+x}]O_4$ and $(Mg_xFe_{1-x})[Mg_{1-x}Fe_{1+x}]O_4$ Spinel Nanoparticles

chemical composition	lattice constant (Å)	cation distribution		atomic displacement U (Å^2)	magnetic moment (μ_B)		goodness of fit reflcn statistics $R(f^2)$
		A site	B site		A site	B site	
$CoFe_2O_4$	8.3816	$Co_{0.31}Fe_{0.69}$	$Co_{0.34}Fe_{0.66}$	0.0072	−3.08	3.21	0.1024
$MgFe_2O_4$	8.3954	$Mg_{0.32}Fe_{0.68}$	$Mg_{0.35}Fe_{0.65}$	0.0085	−2.75	1.51	0.1217

nanoparticles reorients more slowly than 10 ns, Mössbauer spectrometer will be able to observe the magnetic hyperfine interaction and provide a spectrum with a sextet peak. If τ is shorter than 10 ns, the time average for the internal magnetic field created from the magnetic moments at the crystal lattices becomes zero during Mössbauer measurement. The absorption peak in the Mössbauer spectrum will only be a doublet, which corresponds to the quadrupole splitting of nuclear energy levels.[2,27,28]

Figure 6 a,b presents the Mössbauer spectra of $MgFe_2O_4$ and $CoFe_2O_4$ nanoparticles with a size of 20 nm, respectively. At 410 K, the $MgFe_2O_4$ nanoparticles generate a prominent doublet absorption component. When the measuring temperature is lowered to even 300 K, τ of the $MgFe_2O_4$ nanoparticles is still shorter than 10 ns and will not give a single sextet pattern. On the contrary, a single sextet pattern appears at temperatures as high as 400 K in the same size $CoFe_2O_4$ nanoparticles, which implies that τ has already reached 10 ns. According to eq 2, a higher temperature for τ increasing to 10 ns implies a larger K value. Therefore, the Mössbauer spectroscopic studies provide the direct evidence that the anisotropy constant K is much larger in $CoFe_2O_4$ nanoparticles.

The quantum origin of the magnetocrystalline anisotropy is the L−S couplings at crystal lattices, and the anisotropy constant K indicates the strength of such couplings. Certainly, the L−S couplings in Fe^{3+} cations should contribute to the magnetic anisotropy. Since quantum couplings may not be the same at A and B sites with tetrahedral and octahedral symmetries, respectively, the contribution to the magnetic anisotropy from the L−S couplings in Fe^{3+} cations may not be the same when the cation distribution changes. To compare the contributions of Fe^{3+} cations to magnetic anisotropy in $MgFe_2O_4$ and $CoFe_2O_4$ nanoparticles, the cation distribution needs to be identified. Neutron diffraction combined with the Rietveld refinement has been used to determine the cation distribution in $MgFe_2O_4$ and $CoFe_2O_4$ nanoparticles. Figure 7 , parts a and b, displays the neutron diffraction patterns of $MgFe_2O_4$ nanoparticles and $CoFe_2O_4$ nanoparticles, respectively. The structural parameters from the Rietveld refinement of these patterns are listed in Table 1. The $MgFe_2O_4$ nanoparticle has 68% A sites and 65% B sites occupied by Fe^{3+} cations, and the Fe^{3+} cations occupy 69% A sites and 66% B sites in the $CoFe_2O_4$ nanoparticles. The cation distribution is considered the same as in $MgFe_2O_4$ and $CoFe_2O_4$ nanoparticles even though the neutron determination of cation distribution in nanoparticles usually has about 7−8% error margin.[10] The cation distributions in these nanoparticles remain the same in our in situ neutron diffraction studies at elevated temperatures, which indicates that an equilibrium state is achieved for the cation distribution. In addition, the lattice constants in the unit cells of $MgFe_2O_4$ and $CoFe_2O_4$ crystal structures are essentially the same. Therefore, the contribution to E_A from the L−S couplings at Fe^{3+} cation sites is equal in these two types of spinel ferrite nanoparticles.

Hence, the huge difference in the blocking temperature between the same sized $MgFe_2O_4$ and $CoFe_2O_4$ nanoparticles is only due to the switching of chemical component between Mg^{2+} and Co^{2+} cations. The Mg^{2+} cation has no unpaired electrons and therefore zero total electron spin. In the $CoFe_2O_4$ spinel, the Co^{2+} cations have high spin ligand fields and possess seven d electrons with three of them unpaired. Evidently, the larger magnetocrystalline anisotropy E_A of $CoFe_2O_4$ nanoparticles is due to the strong L−S couplings at Co^{2+} cation sites. Therefore, a direct correlation is established between the magnetic anisotropy and the magnetic coupling. The magnetic properties of nanoparticles are connected with the crystal chemistry at the atomic level.

Conclusions

With a significant contribution to the magnetic anisotropy energy barrier by the L−S couplings at Co^{2+} lattice sites, the blocking temperature of $CoFe_2O_4$ nanoparticles is at least 150 deg higher than that for the same sized $MgFe_2O_4$ nanoparticles. Mössbauer spectroscopy studies on the superparamagnetic relaxation of these two types of spinel ferrite nanoparticles confirm that the magnetic anisotropy of $CoFe_2O_4$ nanoparticles is higher than that of the same size $MgFe_2O_4$ nanoparticles. These studies establish the direct correlation between the L−S couplings with the superparamagnetic properties of nanoparticles. Moreover, they elucidate the mechanism for controlling E_A by manipulating the crystal chemistry of nanoparticles, and therefore achieve the variation of the superparamagnetic properties without changing the size of nanoparticles. The results here prove a feasible way for chemical control of superparamagnetic properties in nanoparticles. The ability to design the nanoparticles with or without superparamagnetic properties over a large size range certainly facilitates the applications of magnetic nanoparticles for high-density data storage and for drug delivery using nanoparticulate magnetic carriers.

Acknowledgment. We thank Dr. Bryan Chakoumakos of Oak Ridge National Laboratory for his help in neutron diffraction studies. A.J.R. is partially supported by a Cherry Henry Emerson Chemistry Fellowship. We gratefully acknowledge the financial support in part from NSF (DMR-9875892) and the Beckman Young Investigator program of the Arnold and Mabel Beckman Foundation. The TEM studies were conducted in the Electron Microscopy Center at Georgia Tech. The neutron diffraction studies were carried out at Oak Ridge National Laboratory, which is managed by Lockheed Martin Energy Research Corp. for the U.S. Department of Energy under contract No. DE-AC0596OR22464.

JA000784G

(27) Néel, L. *Ann. Geophys*. **1949**, *5*, 39.
(28) Leslie-Pelecky, D. L.; Rieke, R. D. *Chem. Mater*. **1996**, *8*, 1770.